MALAYSIAN JOURNAL OF INNOVATION IN ENGINEERING AND APPLIED SOCIAL SCIENCE (MyJIEAS)
e-ISSN: 2811-3780
VOLUME 04, ISSUE 01

A Study of 3D Printing for Cosmetic Packaging on Surface Roughness and Water Absorption: Taguchi Approach

Aznifa Mahyam Zaharudin[1,] *, Nurul Amyra Mohd Hishamudin[1] and Muhammad Arif Ab Hamid Pahmi[1]
[1]Mechanical Engineering Studies, College of Engineering, Universiti Teknologi MARA, Penang Branch, Permatang Pauh Campus 13500 Permatang Pauh, Penang, Malaysia

*Corresponding Author's Email: aznifa@uitm.edu.my

Article History: Received 13082024; Revised 22082024; Accepted 04102024;

ABSTRACT – *Cosmetics possessed the potential to develop novel packaging through the utilization of 3D printing, an additive manufacturing (AM) technique that offered advantages over traditional manufacturing methods. This study aimed to optimize the 3D printing process parameters for cosmetic packaging using the Taguchi approach. A cosmetic packaging bottle using polylactic acid (PLA) filament was chosen for 3D printing prototype. The research employed an L9 orthogonal array to investigate the effects of infill density (3%, 5 % and 10 %), infill pattern (cross, triangle and tri-hexagon) and printing speed (30 mm/s, 50 mm/s and 100 mm/s) on surface roughness and water absorption. The optimal parameters for surface roughness were infill density of 5%, a tri-hexagon infill pattern and a printing speed of 50 mm/s. Printing speed displayed the greatest influence on reducing water absorption in the 3D printed parts. The study demonstrates the effectiveness of the Taguchi approach in optimizing 3D printing parameters for cosmetic packaging, ensuring a desirable surface finish, reduced porosity and longevity.*

KEYWORDS: packaging, optimization, 3D printing, surface roughness, water absorption

1.0 INTRODUCTION

3D printing has transformed packaging manufacturing, enabling the creation of unique and customized designs for jars, bottles, and caps. This additive manufacturing (AM) technique enhances brand image and improves the customer experience [1-2]. This technology has facilitated the development of environmentally friendly polymers, and the growing demand for sustainable and durable cosmetic packaging. Traditional packaging often contains greasy chemicals that are difficult to remove and hinder recycling [3]. 3D printing offers packaging and containers to be produced in tailor-made shapes, sizes, and textures that were previously impractical using conventional methods, besides enabling the creation of lightweight, eco- friendly materials and reducing environmental impact [4-6].

The demand for 3D printing in cosmetic packaging has surged due to its versatile applications in the modern era. However, achieving good surface quality and a high-quality end product requires precise control over the 3D printing process parameters. Current research lacked a systematic methodology for optimizing the 3D printing process and exploiting the unique features of PLA material specifically for cosmetic packaging. This gap hindered the identification of critical process parameters and their optimal values necessary to attain desired aesthetic qualities in packaging, such as structural integrity and surface finish.

In 3D printing, a multitude of process parameters dictate the complexities of the printing procedure. These include infill density, infill pattern, printing speed, build orientation, raster angle, raster gap, raster size, raster width, layer thickness, nozzle size, filament size, and more. These parameters greatly impact the precision, efficiency, and properties of the final additive manufacturing products [7]. Careful selection and optimization of these 3D printing process parameters are crucial for achieving high-quality, accurate, and efficient 3D printed components [8].

Plastic filaments used in 3D printing have negatively impacted the environment. The production of waste from unsuccessful prints or rejected support structures has led to a waste management challenge. The increased use of thermoplastic prints due to additive technology advancements has exacerbated the issue. A possible solution lies in utilizing filaments derived from plastic recycling. However, in the case of cosmetic packaging, reusing packaging materials is uncommon. Cinelli et al. [3] highlighted the difficulty of chemical and mechanical recycling due to challenges in collecting post-use packaging and contamination caused by residues from cosmetic products that are hard to remove by washing. Wang et al. [9] conducted research investigating the effects of fused deposition modeling (FDM)-3D printing parameters of nozzle temperature, platform temperature, printing speed, and layer thickness on the mechanical properties and microstructure of carbon fiber (CF) and glass fiber (GF) reinforced heat-resistant polyetheretherketone (PEEK). The study identified the failure reasons of each printed samples for varying printing parameter settings.

Hikmat et al. [10] analyzed tensile strength by varying build orientation, raster orientation, nozzle diameter, infill density, shell number, and extruder speed. Saeed et al. [11] investigated the mechanical properties of continuous carbon fiber-reinforced polyamide polymer composite samples using compression and flexural testing by varying the fiber volume contents by applying pressure, temperature and holding the samples for 60 minutes in the platen press. According to the study, there was a significant relationship between the mechanical and microstructure characteristics of the 3D-printed polymer composites. Hamat et al. [12] employed the Taguchi method of L25 orthogonal array (OA) to investigate the effect of extrusion parameters on the tensile strength quality of 3D printed filament. The research findings revealed that the optimal extrusion temperature and speed for achieving the highest tensile strength with a good filament size of PLA-3D850 were approximately 175℃ and 4 rpm, respectively.

Several observations have been conducted for surface roughness and porosity on 3D printing process parameters. Buj-Corral et al. [13] focused on porosity and pore size analysis, using nozzle diameter and infill percentage meanwhile Alsoufi et al. [14] studied surface roughness by considering nozzle diameter and layer height. Buj-Corral et al. [13] analyzed the effect of nozzle diameter and infill on porosity and pore size of FDM printed specimens with a rectilinear grid pattern where the study showed that the higher infill, the lower porosity, and pore size. Higher nozzle diameter suggests larger pores with comparable porosity. Alsoufi et al. [14] experimentally studied how surface roughness performance of printed parts manufactured by desktop FDM 3D printers with PLA+ is influenced by measuring direction. The findings demonstrated that the component quality finish, build time and final part cost are significantly influenced by the nozzle diameter and layer height. Ranjan et al. [15] investigated the dimensional accuracy and surface roughness of ABS polymer-based 3D printed nuts and bolts. The findings concluded that surface roughness and dimensional analysis have been optimized by stating that ABS-based nuts and bolts are easily made by 3D printing technology.

Therefore, this research aimed to investigate the effect of infill density, infill patterns and printing speed used in 3D printing for producing a prototype of cosmetic packaging on surface roughness and water absorption. To reduce the waste of printing materials when producing cosmetic packaging, the Taguchi method was utilized during the experiment to minimize the number of experiments required.

2.0 METHODOLOGY

The cosmetic packaging design was selected based on an existing product with dimensions of 42 mm in width and 156.8 mm in overall length as shown in Figure 1. The design was reconstructed using Autodesk Fusion 360, a computer software program.

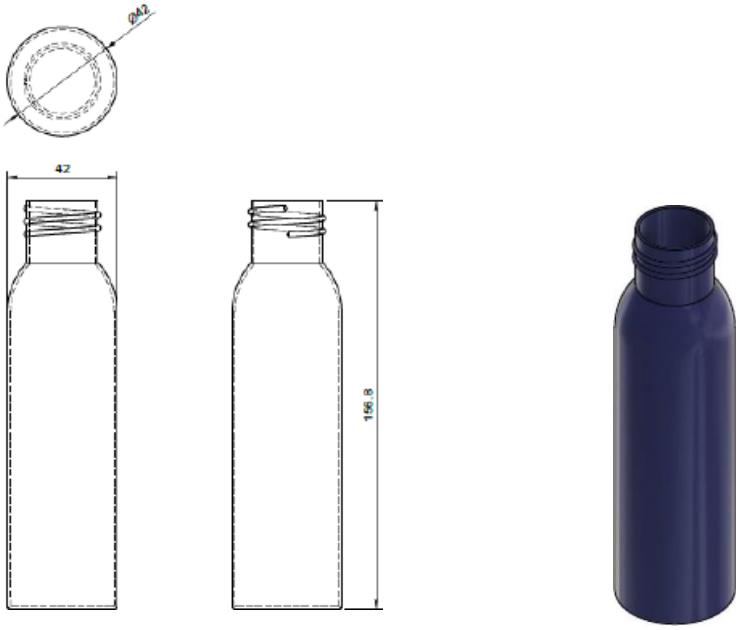

(a) (b)

Figure 1. Lower body part (a) projected view and (b) drawn in Autodesk Fusion 360

Following the completion of the modeling process within the CAD tool, the model prototype needed to be saved and converted into the stereolithography (STL) file format. This format enables accurate reading by the printing software. Ultimaker Cura, a slicer software specifically designed for this purpose, was chosen to convert the model into a series of layers and generate a G-code file. This file contains precise instructions tailored to a specific type of 3D printer, facilitating the printing process.

Polylactic acid (PLA) was utilized in this study as the filament for the 3D printing machine (3D Espresso). G-code instructions were utilized by the 3D printer to construct the model by sequentially depositing layers of melted PLA filament according to the specified cross-sectional layout. Prior to commencing the printing process, it was essential to define and configure parameters such as infill density, infill pattern, and printing speed. 3D Espresso used the fused deposition modeling (FDM) technology as the process to print prototype F where the PLA filament was extruded layer by layer onto the build platform. Design analysis was performed using the Taguchi method in the Minitab Statistical Software. A total of nine experiments were designed according to standard Taguchi's L9 OA, which has nine rows, corresponding to the number of tests, with three factors at three levels (33) as shown in Table 1.

Table 1. The experimental layout of Taguchi L9 orthogonal array

Set	A	B	C
1	3	cross	30
2	3	triangle	50
3	3	tri-hexagon	100
4	5	cross	50
5	5	triangle	100
6	5	tri-hexagon	30
7	10	cross	100
8	10	triangle	30
9	10	tri-hexagon	50

Infill density, infill pattern, and printing speed were selected as the 3D printing parameters to analyze the effects on surface roughness and water absorption. The first column in Table 1 was assigned to infill density (A), the second to infill pattern (B) and the third to printing speed (C). The settings of A include 3% (level 1), 5% (level 2) and 10% (level 3) of infill density. The second factor examined was the infill pattern (B) shown in Figure 2, with options of the cross (level 1), triangle (level 2) and tri-hexagon (level 3). Lastly, the third factor explored was the printing speed (C), with levels of 30 mm/s (level 1), 50 mm/s (level 2) and 100 mm/s (level 3).

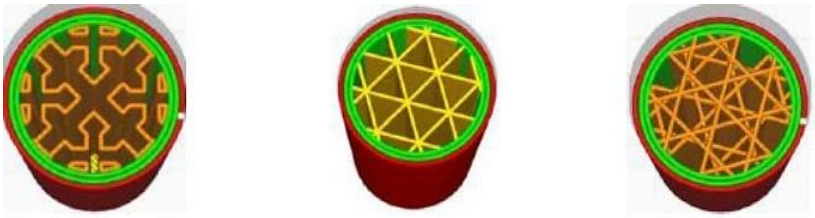

(a) (b) (c)

Figure 2. Different infill pattern (a) cross, (b) triangle, (c) tri-hexagon

The surface roughness experiment was conducted using the SJ410 MITUTOYO, with measurements performed according to the ISO 1997 standard. To determine the water absorption percentage, ASTM D570 (water uptake) was used by immersing the specimen in water for a specified duration. However, a modification was made to the standard water absorption test procedure: instead of fully submerging the prototype in water, water was placed inside the 3D printed prototypes, allowing for 24 24-hour immersion period. To ensure the 3D printed prototypes were free from any pre-existing moisture, the prototypes were subjected to 2424-hour heating process at 30oC in a specimen dryer shown before the immersion. The water absorption was calculated using the given Equation (1),

$$\text{Water Absorption (\%)} = \frac{(wet\ weight - dry\ weight)}{dry\ weight} \text{ X } 100\%$$

where wet weight is the weight of the specimen after immersion (final weight) and dry weight is the weight of the specimen after drying (initial weight).

3.0 RESULTS AND DISCUSSION

Table 2 shows the experimental results of average surface roughness, R_a and water absorption. In this experiment, smaller values of average surface roughness and water absorption amounts were desirable. Set 8 with 10% infill density, triangle infill pattern and 30 mm/s printing speed demonstrated the best surface roughness, with an average roughness value of 9.203 µm. Set 2 with 3% infill density, triangle infill pattern and 5▪0 mm/s speed show the lowest water absorption value of 2.15%. The category the-lower-the-better was used to calculate the S/N ratio for both quality characteristics surface roughness and water absorption, according to Equation (2).

$$S/N = -10log\frac{1}{n}(\sum_{i-1}^{n} y_i^2) \quad (2)$$

Table 2: Experimental results for surface roughness and water absorption

Set	Surface roughness, R_a (μm)	Water absorption (%)
1	9.582	2.70
2	10.116	2.15
3	9.705	2.77
4	9.515	2.28
5	9.802	3.38
6	10.089	2.67
7	9.775	2.50
8	9.203	2.41
9	9.770	2.19

Table 3. Optimum condition by utilizing S/N ratio for surface roughness

Level	Infill Density (%)	Infill Pattern	Printing speed (mm/s)
1	-19.82	-19.67	-19.66
2	-19.82	-19.74	-19.82
3	-19.63	-19.87	-19.79
Delta, Δ	0.20	0.21	0.16
Rank	2	1	3

The analysis of the average surface roughness results leads to the details in Table 3 and Figure 3 which is used to determine the optimal set of parameters from this experimental design. Delta represents the difference between the highest and lowest S/N ratio values for each parameter. A larger delta indicates a more significant impact on the outcome of surface roughness. Infill pattern (Δ = 0.21) appears to have the greatest influence on surface roughness, followed by infill density (Δ = 0.20) and printing speed (Δ = 0.16). The main effect plots in Figure3 also show the infill pattern has the most significant influence on surface roughness, surpassingthe impact of both infill density and printing speed. The main effect plots confirm that the optimal condition identified aligns consistently with the information provided in Table 3. The control factor of infill pattern (B) at level 3 (tri-hexagon) provided the best result. The optimal value for the S/N ratio of 'smaller the better' was obtained through the combination of an infill density of 5%, a tri-hexagon infill pattern and a printing speed of 50 mm/s. These parameters yielded the most desirable minimum surface roughness.

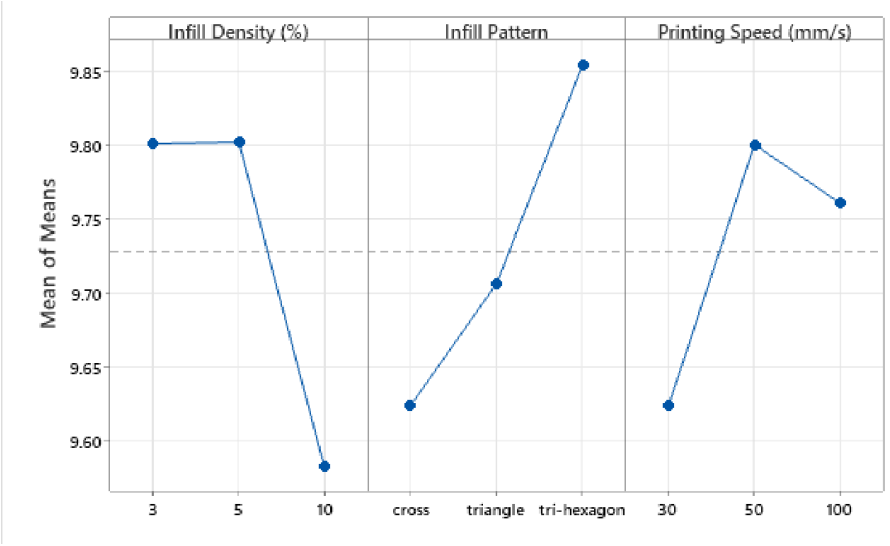

Figure 3. Main effects plot for surface roughness

Table 4: Optimum Condition by Uilizing S/N Ratio for Water Absorption

Level	Infill Density (%)	Infill Pattern	Printing speed (mm/s)
1	-8.045	-7.918	-8.269
2	-8.756	-8.289	-6.872
3	-7.469	-8.063	-9.129
Delta, Δ	1.286	0.371	2.257
Rank	2	3	1

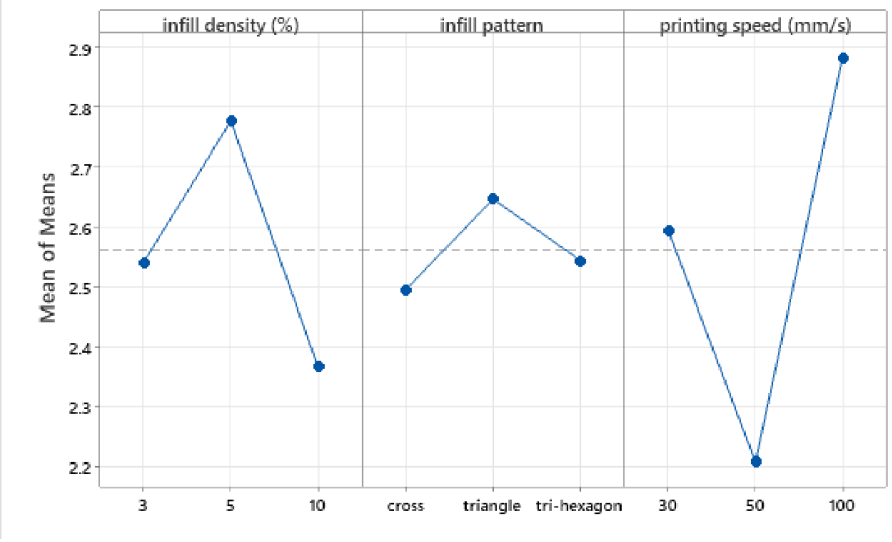

Figure 4. Main effects plot for water absorption

The delta (Δ) values in Table 4 represent the change in water absorption observed when switching between different levels of each factor. Printing speed exhibited the greatest influence on reducing water absorption in the 3D printed parts. This is evident from its corresponding delta value (Δ = 2.257), which is the highest value in Table 4. Since lower water absorption is generally associated with lower porosity in materials, it can be inferred that the printing speed factor significantly contributes to reducing porosity. Consequently, using a higher printing speed during fabrication likely results in denser parts with diminished porosity, potentially enhancing the characteristics of cosmetic packaging by improving factors like barrier properties or product shelf life. The optimized combination of levels for the three control factors from the analysis of water absorption shown in Figure 4 was 5% of infill density, triangle infill pattern and 100 mm/s of printing speed.

4.0 CONCLUSION

In conclusion, the Taguchi optimization method was effectively utilized to determine the optimal 3D printing parameters for PLA cosmetic packaging. By analyzing surface roughness and water absorption, infill density and infill pattern as critical factors for achieving a smooth surface and low porosity, respectively. This study provides valuable insights for the cosmetic packaging industry, enabling the production of high-quality, functional PLA packaging with desirable aesthetics and minimal product absorption.

REFERENCES

[1] J. Rydz, W. Sikorska, M. Musiol, H. Janeczek, J. Włodarczyk, M. Misiurska-Marczak, J. Lęczycka, and M. Kowalczuk, "3D-Printed Polyester-Based Prototypes for Cosmetic Applications-Future Directions at the Forensic Engineering of Advanced Polymeric Materials", *Materials*, *12*(6), 994., 2019.

[2] C. Langdon, J. Hinojosa-Bernal, J. Munuera, M. Gomez-Chiari, O. Haag, A. Veneri, A. Valldeperes, A. Valls, N. Adell, V. Santamaria, O. Cruz-Martinez, and A. Morales-La Madrid, "3D Printing as Surgical Planning and Training in Pediatric Endoscopic Skull Base Surgery - Systematic Review and Practical Example", *International Journal of Pediatric Otorhinolaryngology*, 168, 111543., 2023.

[3] P. Cinelli, M. B. Coltelli, F. Signori, P. Morganti, and A. Lazzeri, "Cosmetic Packaging to Save the Environment: Future Perspectives", *Cosmetics*, 6(26): 1–14., 2019.

[4] Y. Jiao, M. Stevic, A. Buanz, M. J. Uddin, and S. Tamburic, "Current and Prospective Applications of 3D Printing in Cosmetics: A Literature Review," *Cosmetics*, 9(115): 1–24., 2022.

[5] E. O.Ahaiwe, and U. Ndubuisi, "The Effect of Packaging Characteristics on Brand Preference for Cosmetics Products in Abia State, Nigeria," *British Journal of Marketing Studies*, 3(8): 79–90., 2015.

[6] M. Javaid, A. Haleem, R. Singh, R. Suman, and S. Rab, "Role of Additive Manufacturing Applications Towards Environmental Sustainability," *Advanced Industrial and Engineering Polymer Research*, 4: 312-322., 2021.

[7] K. Srinivasulu Reddy, and S. Dufera, Additive Manufacturing Technologies, *International Journal of Management, Information Technology and Engineering*, 4(7): 89–112., 2019.

[8] M. Manoj Prabhakar, A. K. Saravanan, A. Haiter Lenin, I. Jerin leno, K. Mayandi, and P. Sethu Ramalingam, "A Short Review on 3D Printing Methods, Process Parameters and Materials," *Materials Today: Proceedings*, 45: 6108–6114., 2021.

[9] P. Wang, B. Zou, S. Ding, L. Li, and C. Huang, "Effects of FDM-3D Printing Parameters on Mechanical Properties and Microstructure of CF/PEEK and GF/PEEK," *Chinese Journal of Aeronautics*, 34(9): 236–246., 2021.

[10] M. Hikmat, S. Rostam, and Y. M. Ahmed, "Investigation of Tensile Property-Based Taguchi Method of PLA Parts Fabricated by FDM 3D Printing Technology," *Results in Engineering*, 11, 100264., 2021.

[11] K. Saeed, A. McIlhagger, E. Harkin-Jones, C. McGarrigle, D. Dixon, M. Ali Shar, A. McMillan, and E. Archer, "Characterization of Continuous Carbon Fibre Reinforced 3D Printed Polymer Composites with Varying Fibre Volume Fractions," *Composite Structures*, 282, 115033., 2022.

[12] S. Hamat, M. Ishak, S. M. Sapuan, N. Yidris, M. S. Hussin, and M. S. Manan, "Influence of Filament Fabrication Parameter on Tensile Strength and Filament Size of 3D Printing PLA-3D850," *Materials Today: Proceedings*, 74: 457-461., 2023.

[13] I. Buj-Corral, A. Bagheri, A. Domínguez-Fernández, and R. Casado-López, Influence of Infill and Nozzle Diameter on Porosity of FDM Printed Parts with Rectilinear Grid Pattern, *Procedia Manufacturing*, 41: 288–295., 2019.

[14] M. S. Alsoufi, and A. E. Elsayed, "How Surface Roughness Performance of Printed Parts Manufactured by Desktop FDM 3D Printer with PLA+ is Influenced by Measuring Direction," *American Journal of Mechanical Engineering*, 5(5): 211–222., 2017.

[15] N. Ranjan, "Dimensional and roughness analysis of ABS polymer-based 3D printed nuts and bolts", *Materials Today: Proceedings*, 48: 1604–1608., 2022.